Supporting Information

1300 nm Absorption Two-Acceptor Semiconducting Polymer Nanoparticles for NIR-II Photoacoustic Imaging System Guiding NIR-II Photothermal Therapy

Wansu Zhang, [a, †] *Xiaoli Sun,* [a, †] *Ting Huang,* [a] *Xiaoxia Pan,* [b] *Pengfei Sun,* *[a] *Jiewei Li,* [c] *Hua Zhang,* [a] *Xiaomei Lu,* *[c] *Quli Fan,* *[a] *and Wei Huang* [d]

[a] Key Laboratory for Organic Electronics and Information Displays & Institute of Advanced Materials (IAM), Jiangsu National Synergetic Innovation Center for Advanced Materials (SICAM), Nanjing University of Posts & Telecommunications, 9 Wenyuan Road, Nanjing 210023, China.

[b] State Key Laboratory of Molecular Engineering of Polymers & Department of Macromolecular Science, Fudan University, 220 Handan Road, Shanghai 200433, People's Republic of China

[c] Key Laboratory of Flexible Electronics (KLOFE) & Institute of Advanced Materials (IAM), Jiangsu National Synergetic Innovation Center for Advanced Materials (SICAM), Nanjing Tech University (NanjingTech), 30 South Puzhu Road, Nanjing 211816, China.

[d] Shaanxi Institute of Flexible Electronics (SIFE), Northwestern Polytechnical University (NPU), 127 West Youyi Road, Xi'an 710072, Shaanxi, China.

* E-mail: iamqlfan@njupt.edu.cn

* E-mail: iampfsun@njupt.edu.cn

* E-mail: iamxmlu@njtech.edu.cn

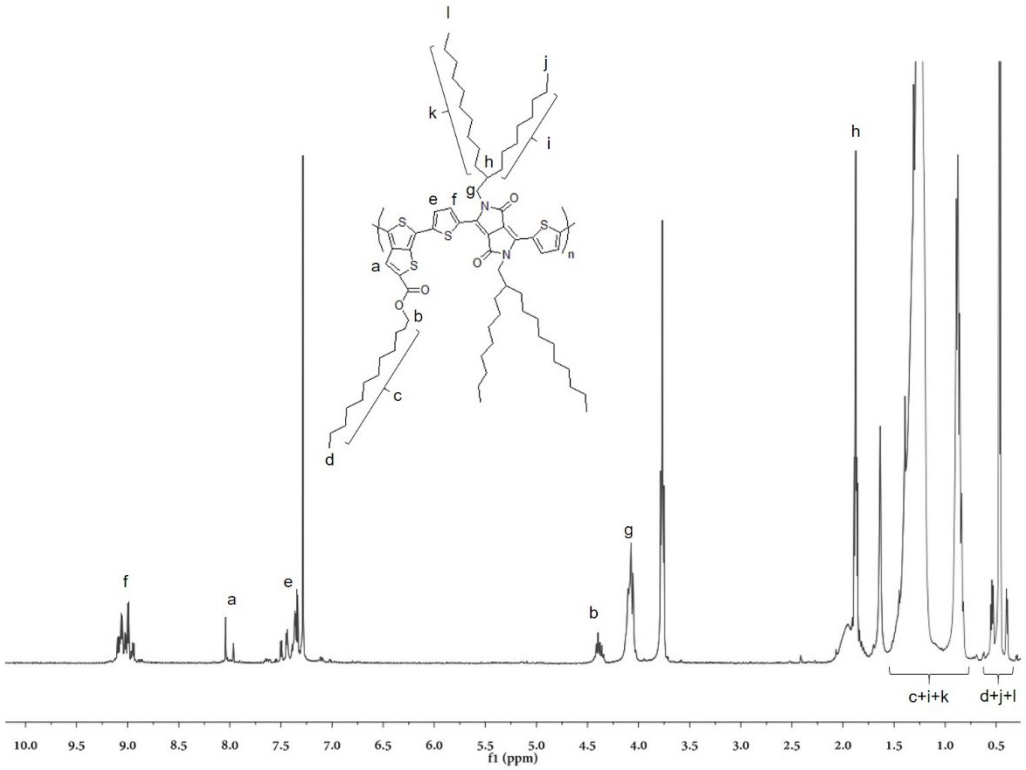

Fig. S1 ^{1}H NMR Spectrum of SP1 in $CDCl_3$.

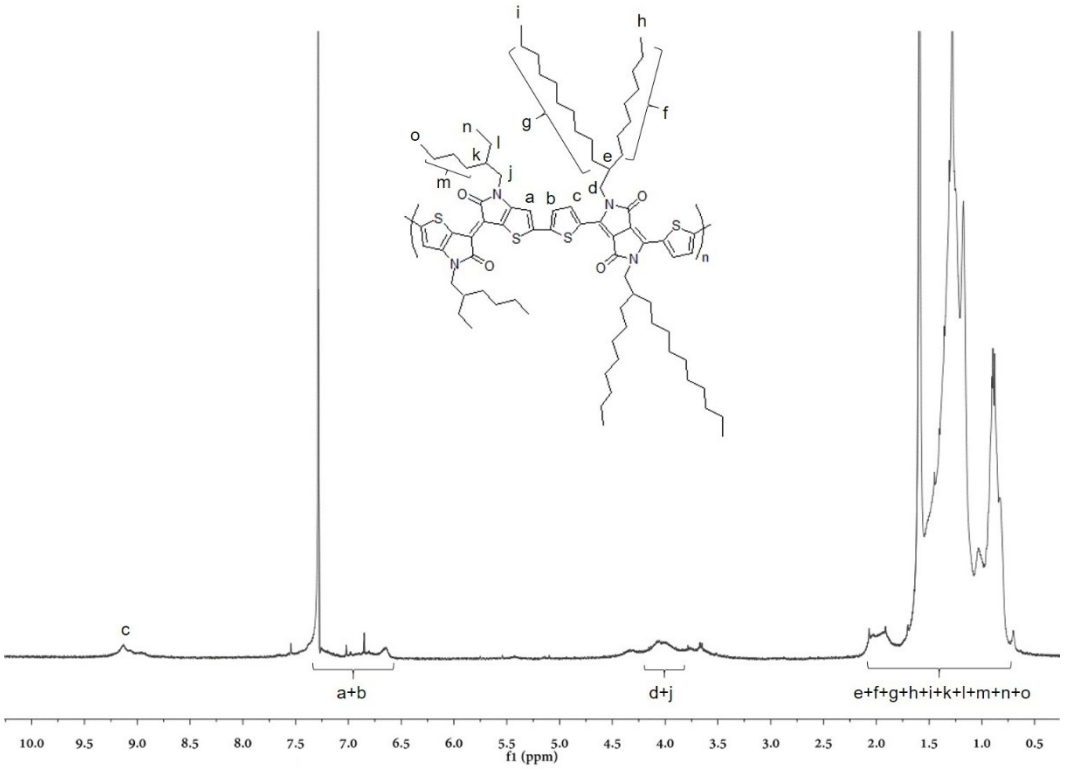

Fig. S2 ^{1}H NMR Spectrum of SP2 in $CDCl_3$.

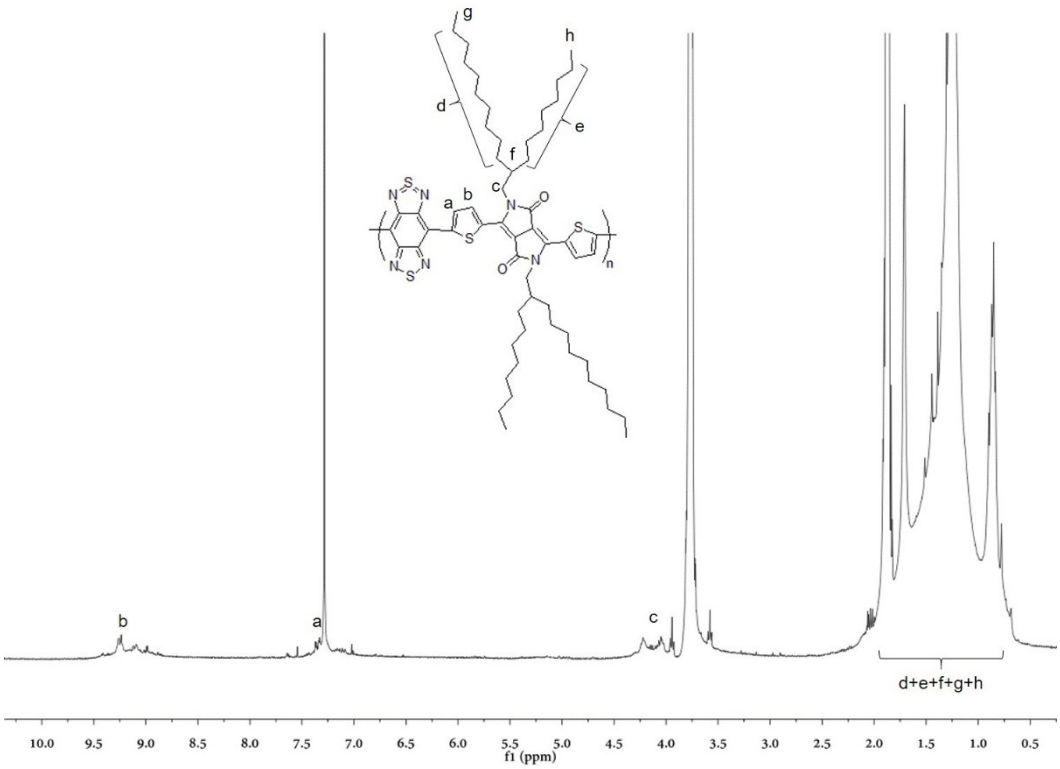

Fig.S3 ^{1}H NMR Spectrum of SP3 in $CDCl_3$.

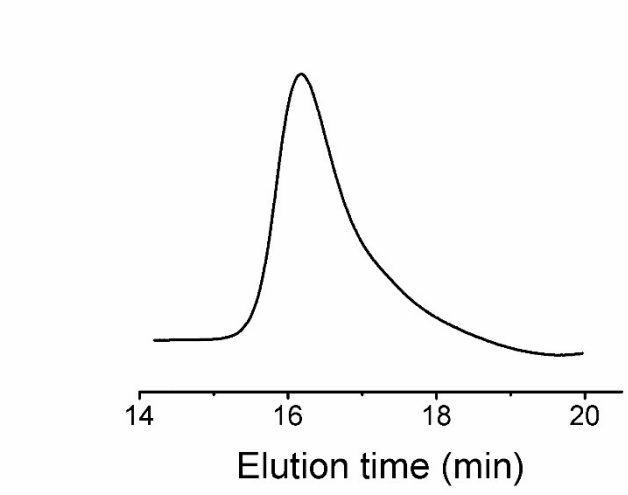

Fig.S4 The GPC curve of SP1.

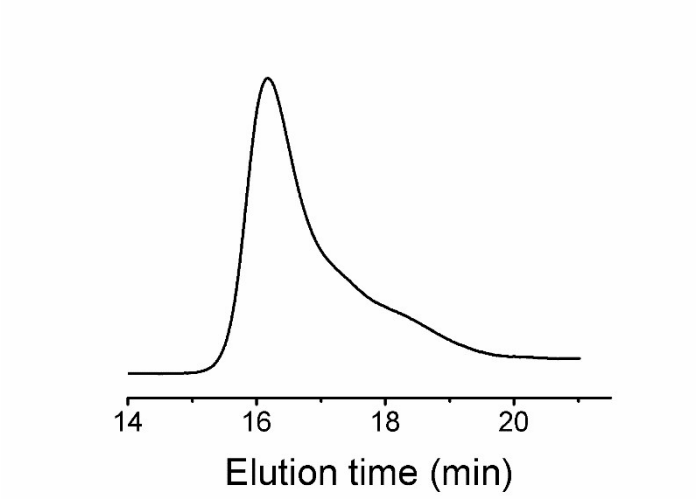

Fig.S5 The GPC curve of SP2.

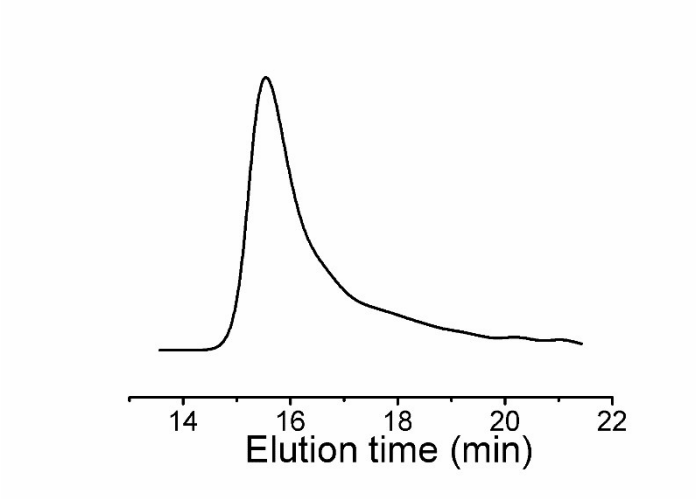

Fig.S6 The GPC curve of SP3.

Table. S1 Comparison of HOMOs and LUMOs orbital surfaces of SP1, SP2 and SP3 using DFT method. To reduce the computational cost, R substituent groups were replaced by methyl, $E_{gap} = E_{LUMO} - E_{HOMO}$

polymer	HOMO	Energy (eV)	LUMO	Energy (eV)	E_{gap} (eV)
SP1	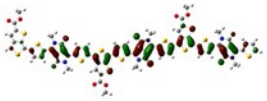	-4.65	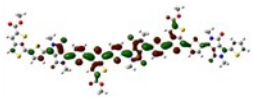	-3.26	1.39
SP2		-4.58	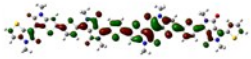	-3.24	1.33
SP3		-4.59	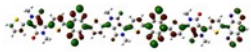	-4.05	0.53

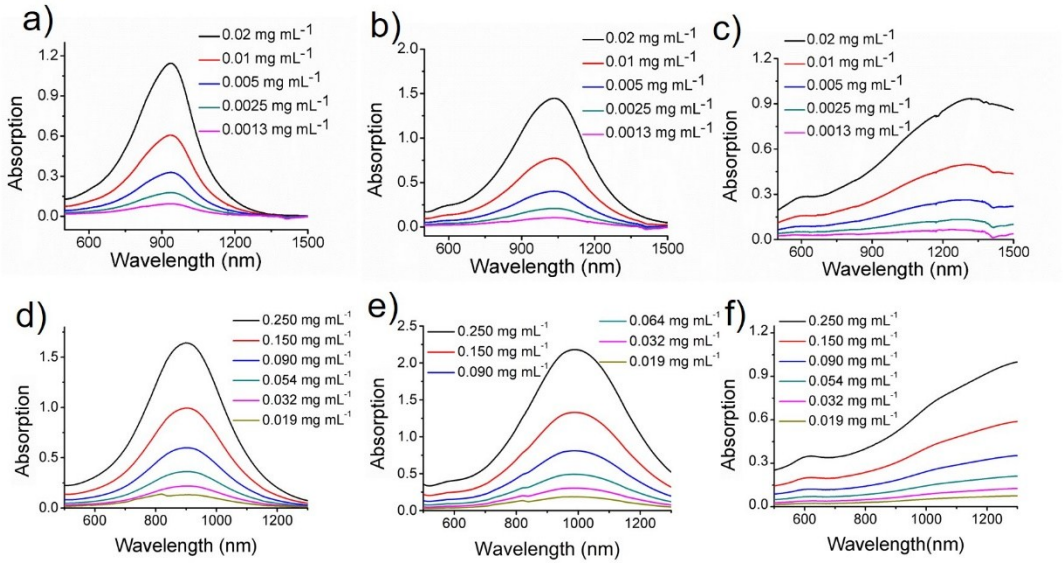

Fig. S7 (a-c) UV−vis-NIR spectra of SP1-3 in THF at different concentrations. (d-f) Absorption spectra of SPNs1-3 in water at different concentrations.

The molar extinction coefficients of SP1-3 were calculated to be 9.0×10^4, 1.0×10^5 and 5.0×10^4 M^{-1} cm^{-1}, respectively, at their maximum absorption peak based on repeating unit molar concentration. For comparison of the PTT effects, the molar extinction coefficient of SP1 was calculated to be 6.9×10^4 M^{-1} cm^{-1} at 915 nm and 3.0×10^4 M^{-1} cm^{-1} at 1064 nm, when the molar extinction coefficients of SP2 and SP3 were calculated to be 9.8×10^4 and 3.8×10^4 M^{-1} cm^{-1} at 1064 nm, respectively. Besides, for comparison of the NIR-II PA property, the molar extinction coefficients of SP1-3 were calculated to be 2.0×10^3, 2.0×10^4 and 5.0×10^4 M^{-1} cm^{-1} at 1300 nm, respectively.

In addition, the molar extinction coefficient of SP2 was calculated to be 4.5×10^4 M^{-1} cm^{-1} at 1200 nm.

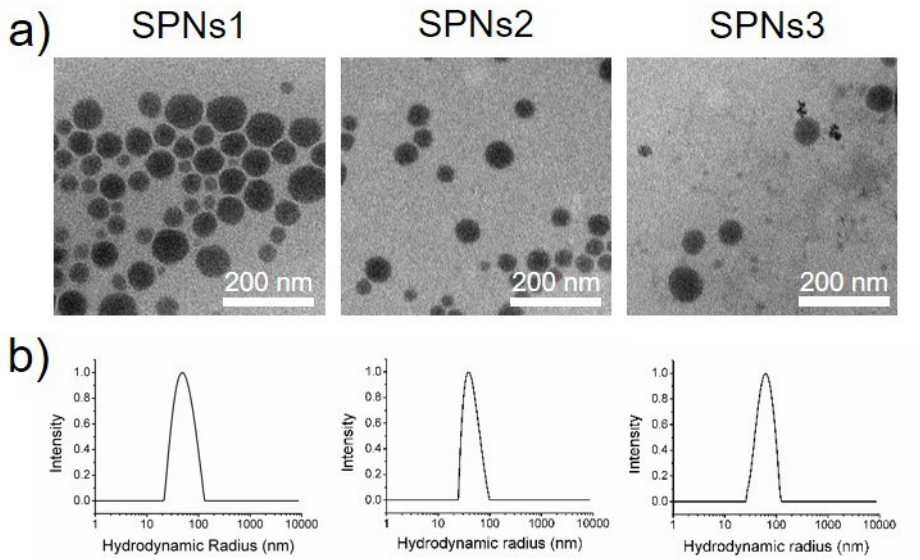

Fig. S8 (a) Transmission electron microscopy images of SPNs1-3, scale bars represent 200 nm. (b) The hydrodynamic radius ($\langle R_h \rangle$) analysis of the three SPNs in water measured by dynamic light scattering (DLS).

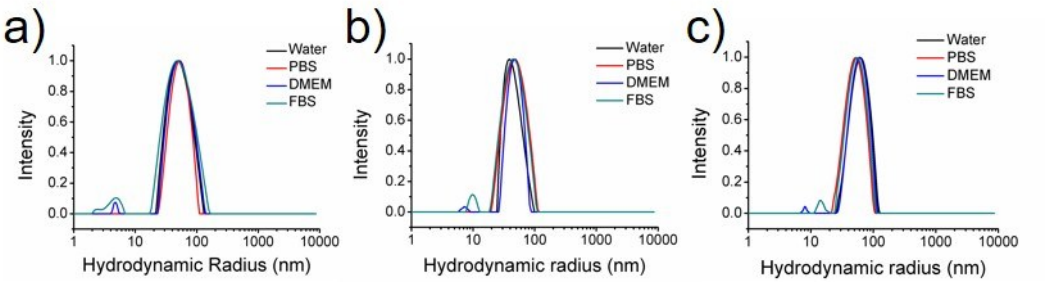

Fig. S9 The hydrodynamic radius ($\langle R_h \rangle$) of SPNs1 (a), SPNs2 (b) and SPNs3 (c) in water, PBS, DMEM and FBS.

As shown in Fig. S9, the three SPNs could be well dispersed in phosphate-buffered saline (PBS), foetal bovine serum (FBS) and Dulbecco's minimum essential medium (DMEM) cell culture medium solution and no aggregation were found in these solution (Fig. S9). These data indicate the SPNs have good chemical and physiological stability for *in vivo* imaging applications.

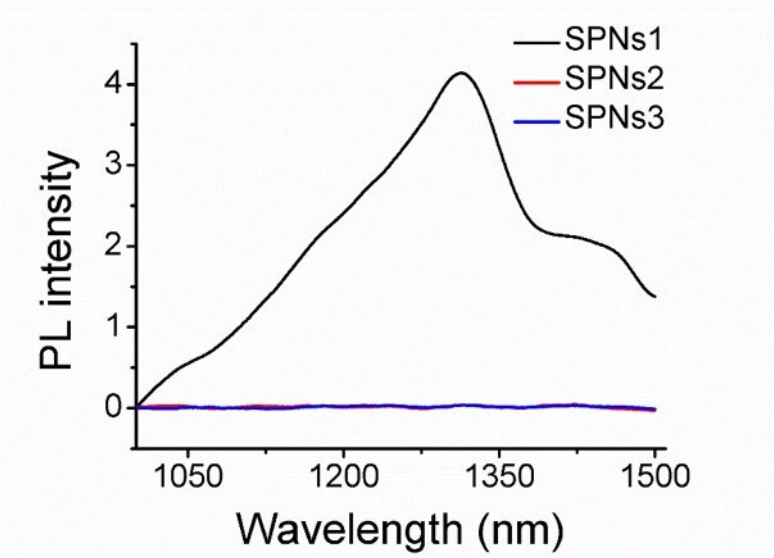

Fig. S10 Emission spectra of SPNs1-3 in water excited by 915 nm laser.

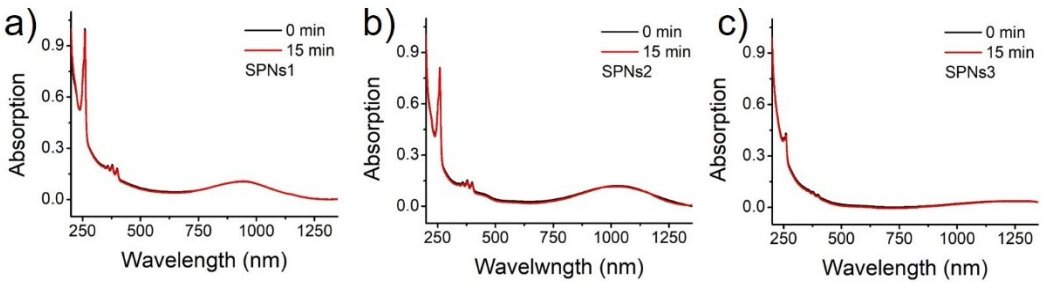

Fig. S11 ROS evaluation of SPNs1-3 (0.01 mg mL^{-1}). Absorption spectra of ABDA and SPNs1-3 mixture under different NIR laser irradiation (0.5 W cm^{-2}) for 1 h: (a) SPNs1 under 915 nm laser, (b) SPNs1 under 1064 nm laser, (c) SPNs3 under 1064 nm laser.

The fluorescence spectrum of SPNs1-3 in water were measured by excitation with a 915 nm laser (Fig. S10). At the same mass concentration, the fluorescence signals of SPNs1 emitted 142 and 174 times stronger than SPNs2 and SPNs3, respectively. In addition, any obvious reactive oxygen (ROS) species had been hardly detected from these three SPNs generated by continuous 915 nm laser irradiation (Fig. S11). Both the low emission and negligible ROS production of SPNs2 and SPNs3 indicated that these two SPNs would produce stronger photothermal effect than SPNs1 since photothermal effect competed with fluorescence emission and ROS production.[1, 2]

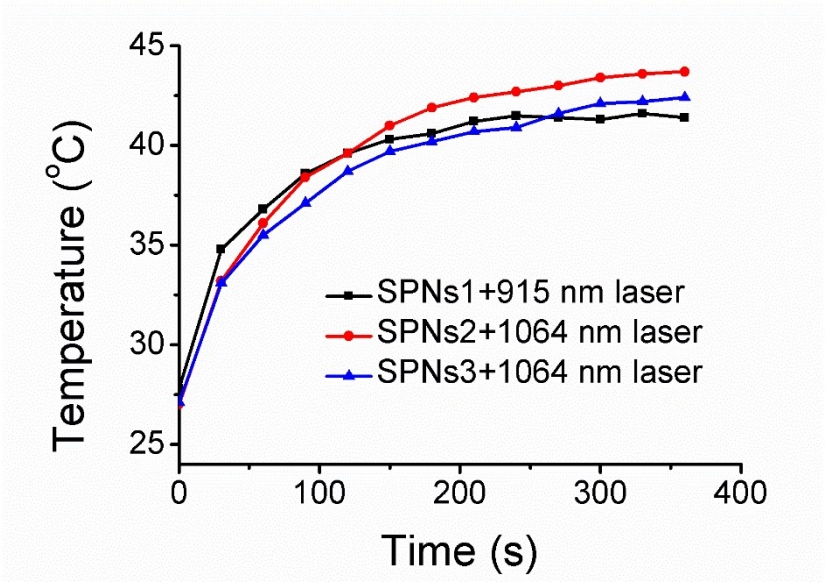

Fig. S12 The temperature change curves of SPNs1-3 at the same concentration after 915 or 1064 nm lasers irradiation at the power intensity of 0.5 w cm^{-2}.

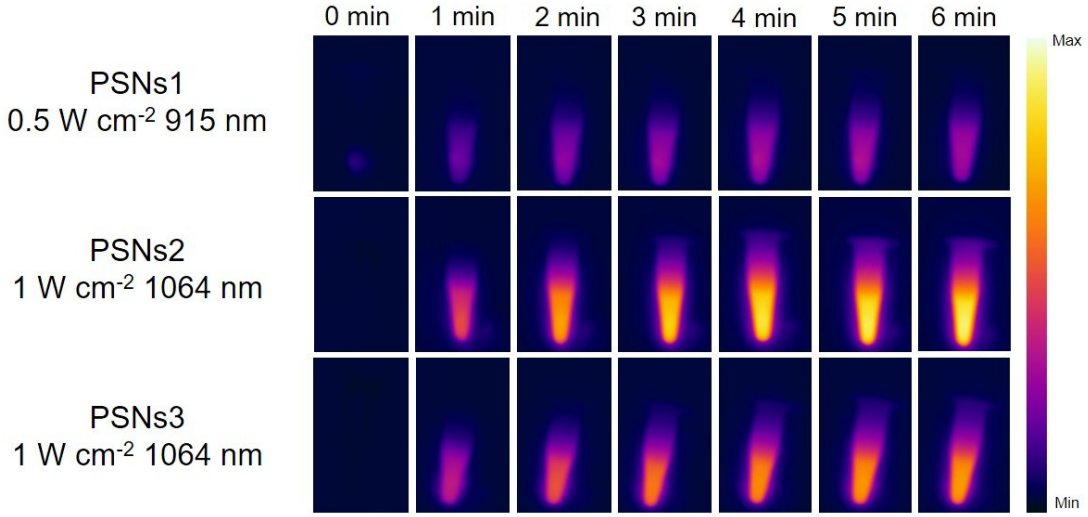

Fig. S13 The thermal images of SPNs1-3 aqueous solution with different concentrations under 915 nm or 1064 nm laser at their MPE limits.

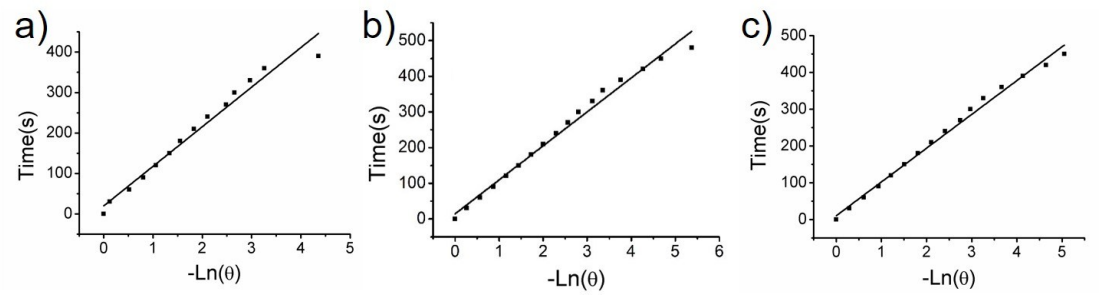

Fig. S14 Calculation of the photothermal-conversion efficiency of SPNs1-3 at 915 nm or 1064 nm. Time constant (τ_s) of SPNs1 (a), SPNs2 (b) and SPNs3 (c) for the heat transfer from the system determined by applying the linear time data from the cooling period.

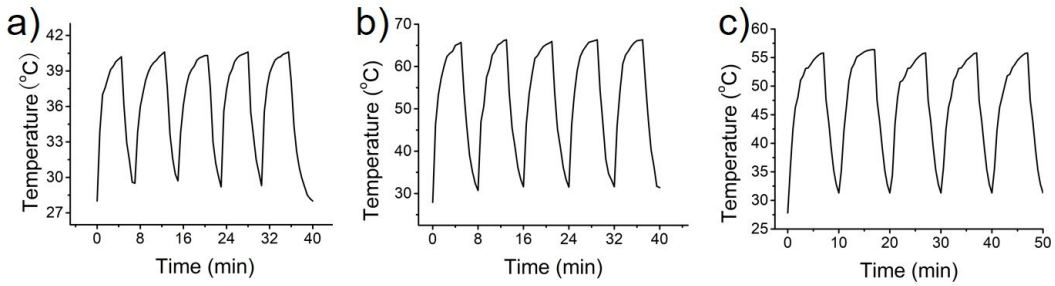

Fig. S15 The photothermal stability of SPNs1-3 aqueous solution. (a) The thermal cycling of SPNs1 (915 nm, 0.5 W cm^{-2}); (b) the thermal cycling of SPNs1-3 (1064 nm, 1 W cm^{-2}); (c) the thermal cycling of SPNs3 (1064 nm, 1 W cm^{-2}).

After five cycles of heating and cooling, the temperature increases of the SPNs solution remained almost the same level, suggesting that the SPNs have excellent photothermal stability for biomedical application (Fig. S15).

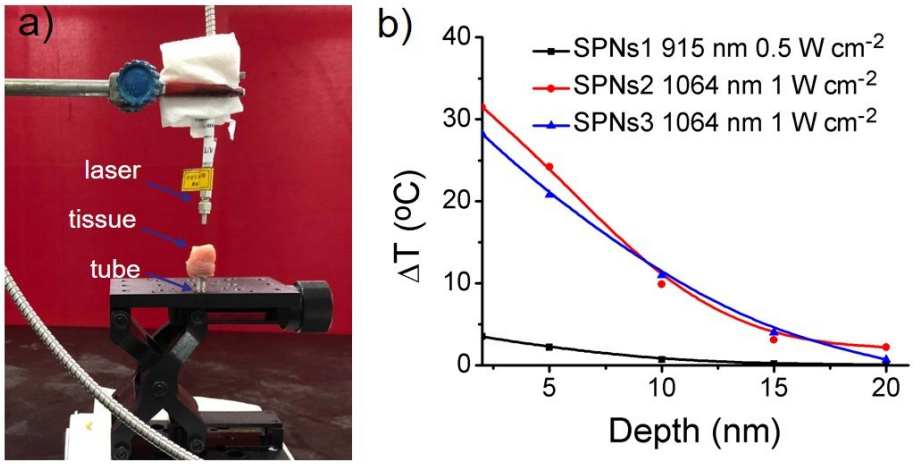

Fig. S16 (a) Photograph of the deep-tissue NIR-II PTT experimental samples setup. The tube was placed under chicken-breast tissue layers. (b) Fitted temperature change curves of SPNs solutions (50 μg mL^{-1}) at different depths of chicken breast tissue under MPE limit laser conditions.

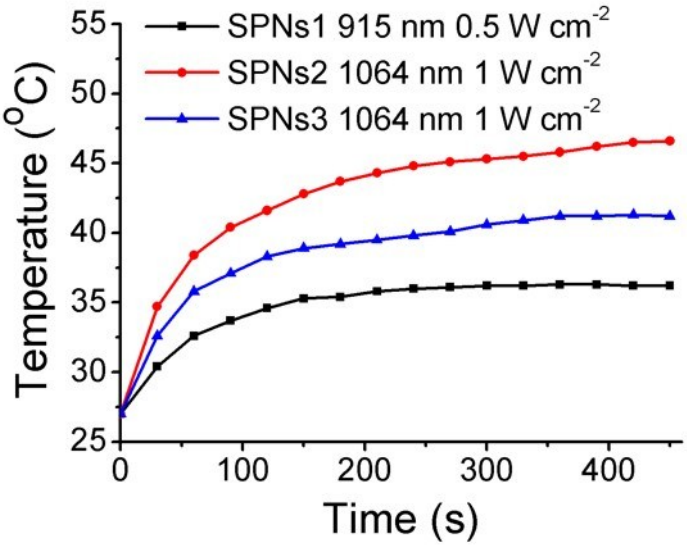

Fig. S17 Deep tissue photothermal heating effects of SPNs under different laser. The mice bearing xenograft 4T1 tumors on the right armpit were intratumorally injected with SPNs1-3 (50 μL, 200 μg mL^{-1}), respectively. A piece of 2 mm chicken breast tissue was placed on top of the tumor during laser irradiation.

The *in vivo* deep-tissue PTT effects of SPNs under 915 or 1064 nm irradiation at their MPE limit were evaluated. As shown in Fig. S17, the temperature change of SPNs were obtained through various laser irradiation upon the tumor surrounded by a piece of 2 mm chicken breast tissue after intratumoral injection of SPNs into the nude mice bearing 4T1 xenograft tumor. After continuous laser irradiation for 450 s, temperature of the tumors with injections of SPNs2 reached the maximum as 46.6 °C higher than SPNs1 (36.2 °C) and SPNs3 (41.8 °C). Interestingly, the *in vivo* deep-tissue PTT effect of SPNs2 was above the PTT temperature threshold required to induce apoptosis of cancer cells (43 °C) .[3] These data confirmed that SPNs2 and SPNs3 under 1064 nm laser irradiation was superior over SPNs1 under 915 nm irradiation for deep-tissue PPT, which was consistent with the *in vitro* results (Fig. 1e).

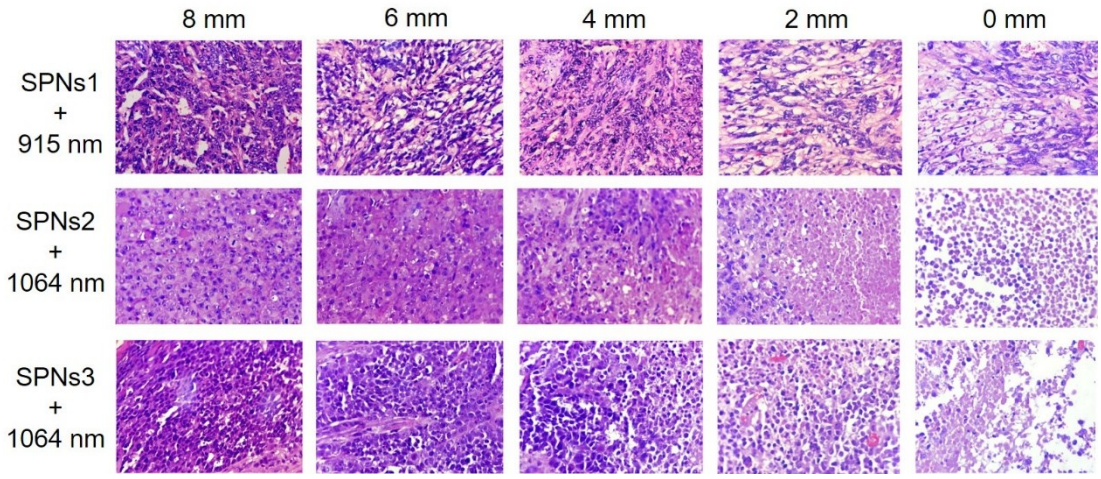

Fig. S18 H&E staining analysis of dissected tumor tissues at different depths (0, 2, 4, 6 and 8 mm) after different treatment.

Furthermore, three groups of 4T1-tumor-bearing mice were intravenously injected with SPNs1-3 solutions (10 mg kg^{-1}), respectively. The tumor sections were irradiated by 915 or 1064 nm lasers under their MPE limit power density for 5 min and then dissected for hematoxylin and eosin (H&E) staining analysis. After the different treatment, the *in vivo* PTT deep-tissue ablation effect of SPNs1-3 were estimated by the H&E staining analysis of the cells at different depths inside the tumor tissues. As shown in Fig. S18, the effective PTT ablation depth of tumor using SPNs2 and SPNs3 under 1064 nm irradiation could achieve almost 4 mm, while 2 mm depth of tumor tissues treated with SPNs1 under 915 nm laser irradiation had no damage. The data implied that the PTT tissue penetration of SPNs2 and SPNs3 exceeded that of SPNs1 similar with the above-mentioned deep-tissue PTT results of SPNs1-3 by the first methods.

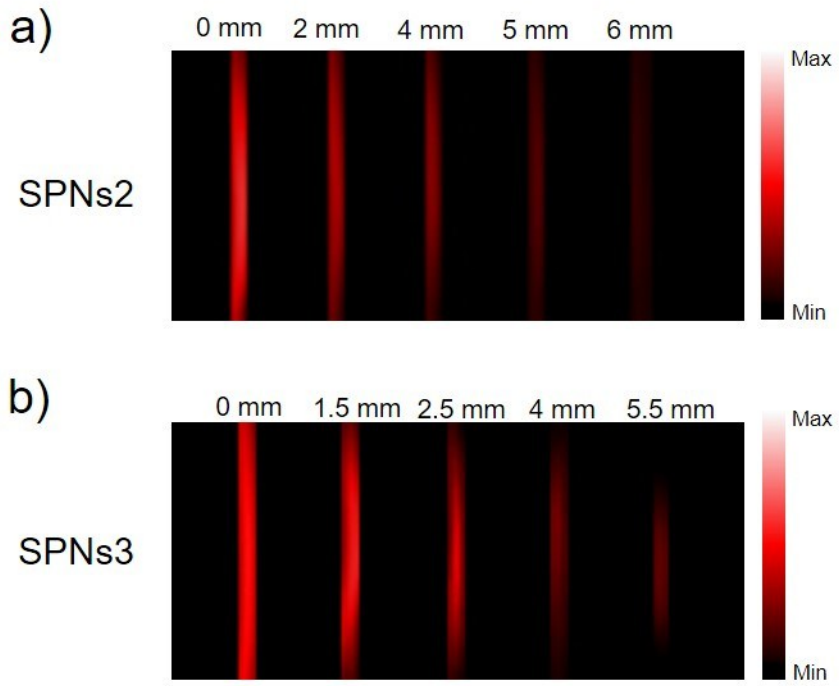

Fig. S19 NIR-II PA images of 1 mg mL^{-1} SPNs2 (a) and SPNs3 (b) at different depths.

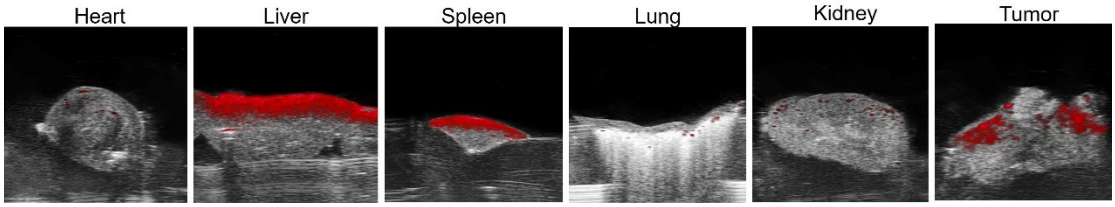

Fig. S20 The PA coronal images of major organs after 1 day SPNs3 injection.

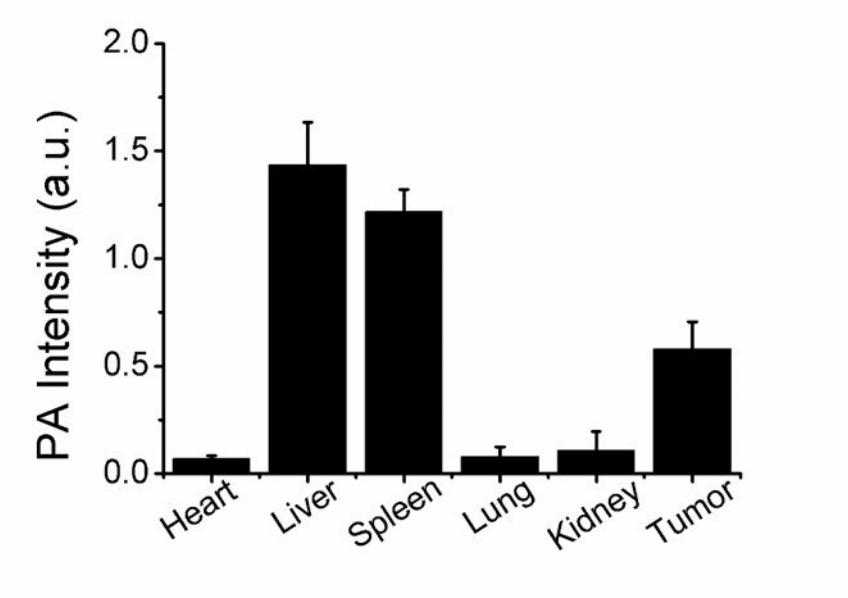

Fig. S21 Quantitative NIR-II PA signals of tumor and main organs after 24 h injection of SPNs3.

Ex vivo biodistribution images and quantitative NIR-II PA intensity of major organs were investigated at 24 h post-injection (Fig. S20 and S21). The considerable PA signals were detected in the liver and spleen, manifesting the clearance by the reticuloendothelial system consistent with many nanoparticle. [50] In addition, strong probe signal was also detected in tumor, indicating that SPNs3 can passively target tumor and be applied to NIR-II PA imaging-guided photothermal therapy.

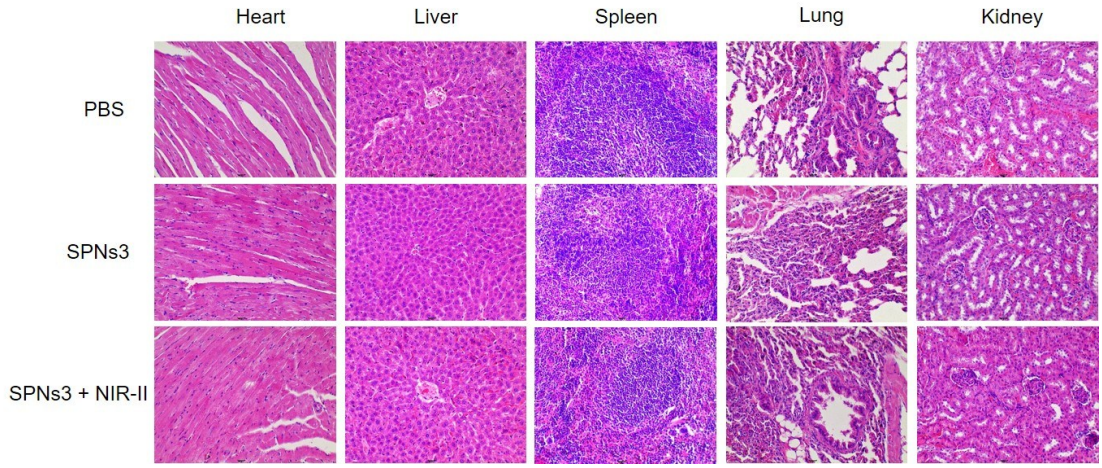

Fig. S22 Hematoxylin and eosin (H&E) co-stained histological analysis of several organs from three groups (PBS, SPNs3 only and SPNs3 + NIR-II)

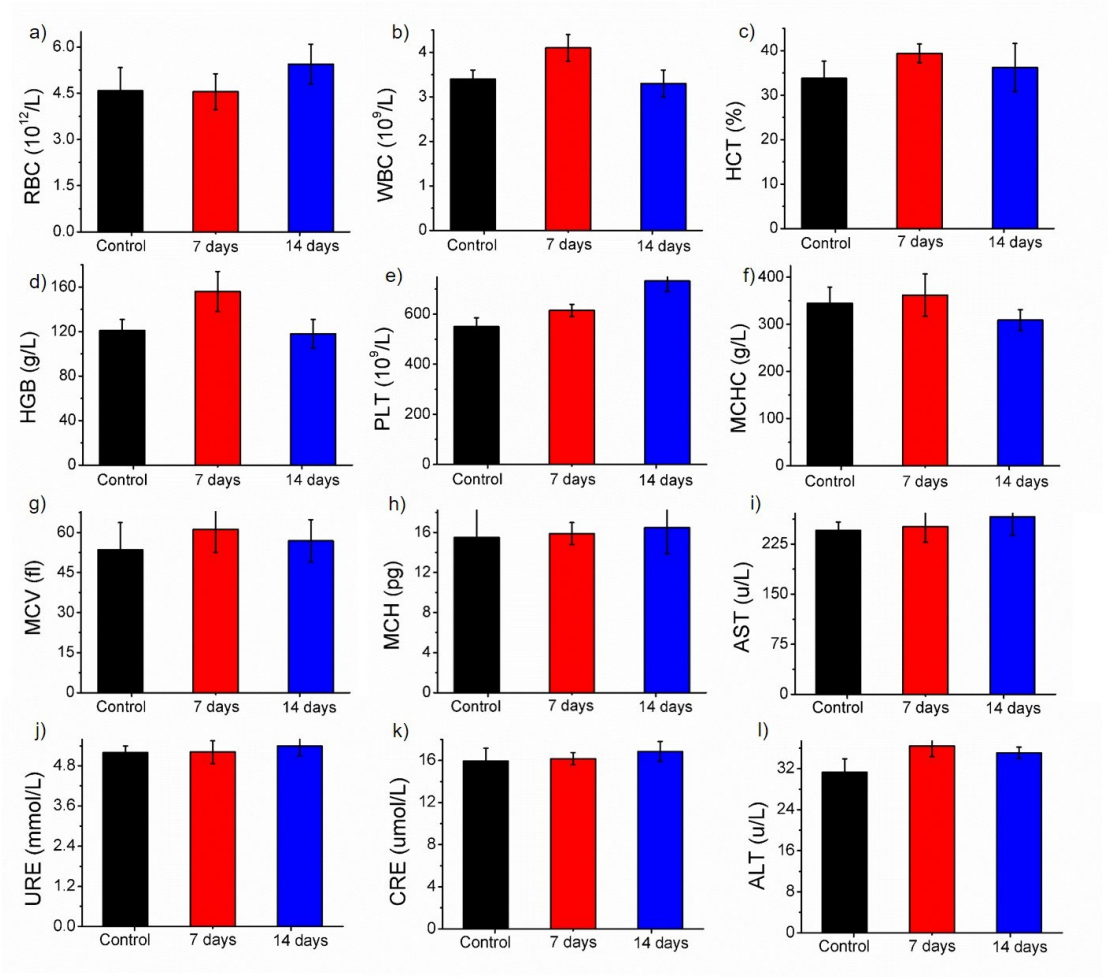

Fig. S23 (a-h) Hematological index of the mice (n = 3) with intravenous administration of 1 mg mL^{-1} SPNs3 during 14 days. The terms include WBC, RBC, HCT, HGB, PLT, MCHC, MCV and MCH. (i-l) Biochemical blood analysis of the TT-3T CPs-treated mice at 7 and 14 days postinjection. The results show the mean and SD of AST, URE, CRE and ALT.

Healthy Balb/c mice (n = 3) were *i.v.* injected with SPNs3 (1 mg mL^{-1}, 150 μL) to assess the in vivo detailed physiological toxicology. The normal hematology parameters including white blood cells, red blood cells, hematocrit, hemoglobin (HGB), platelets, mean corpuscular HGB concentration, mean corpuscular volume, and mean corpuscular HGB were measured (Fig. S23), and the data showed no meaningful changes for SPNs3-treated groups in these indicators over a period of 14 days in comparison with the values of the untreated group. The standard blood biochemical indexes including aspartate aminotransferase (AST), urea, creatinine, and alanine ALT were also examined (Fig. S23). No significant hepatic and renal disorders in the SPNs3-

treated group were found after 7 and 14 days. These results demonstrate that the SPNs3 induced no significant inflammation or infection and no obvious hepatic and renal disorders in the treated group.

EXPERIMENTAL SECTION

Materials

All polymeric synthetic monomers were used as received without any purification. 4,6-Dibromothieno[3,4-b]thiophene-2-carboxylate (1), 2,2'-dibromo-4,4'-bis(2-ethylhexyl)-[6,6'-bithieno[3,2-b]pyrrolylidene]-5,5'(4H,4H')-dione (TIIG) (2) and 4,8-dibromo-benzo[1,2-c;4,5-c] bisthiadiazole (3) were purchased from SunaTech Inc. 3,6-Bis(5-trimethylstannanyl-2-thienyl)-2,5-bis(2-hexyldecyl)pyrrolo-[3,4c]pyrrole-1,4 (2H,5H)-dione (4) was ordered from JiangSu GR-Chem Biotech Co.,Ltd. Tris(dibenzylideneacetone)dipalladium(0) (5) and triphenylphosphine (6) were purchased from J&K Scientific LTD. Pluronic F-127 was obtained from Sigma-Aldrich Chemical Co. Toluene were dried and distilled under a nitrogen atmosphere before synthesis.

Synthesis of Semiconducting polymer SP1

Monomer 1 (0.1 mmol, 51 mg), monomer 4 (0.1 mmol, 118.7 mg) and compound 6 (5.0 mg, 19 μmol) were added in a schlenk tube (10 ml) and dissolved with anhydrous toluene (3 mL). Then catalyzer 5 (2.75 mg, 3.0 μmol) was added in it and the solution was deoxidized with nitrogen for 25 min. The reaction system was stirred at 100 ℃ under nitrogen atmosphere in dark . After 12 h, the mixture was cooled down to room temperature. Then, the reaction solution was precipitated in methanol and collected by filtration. Finally, the resulting polymer were dried under a vacuum to obtain the SP1 (86.9 mg, 70% yield), as the dark blue solid.

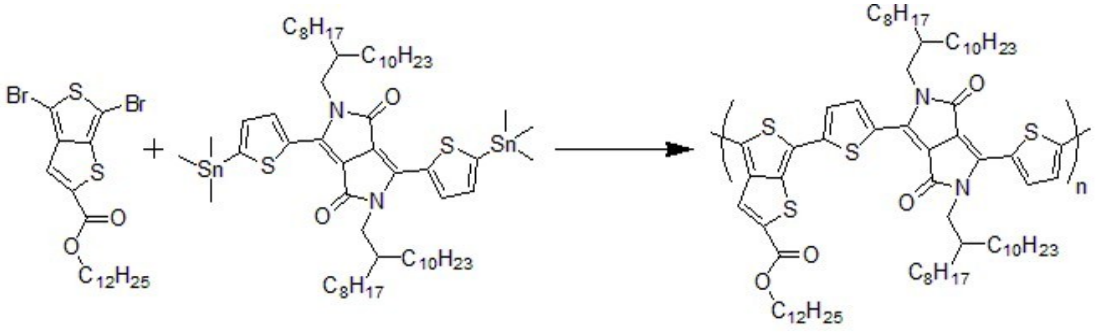

Scheme S1 The synthetic route of SP1.

Synthesis of Conjugated Copolymer SP2

As abovementioned method, same procedure for SP2 was used except monomer 4 (0.1 mmol, 118.7 mg) as one monomer and monomer 2 (0.1 mmol, 65.4 mg) as another monomer. The resulting polymer SP2 was dark green solid, yield: 97.2 mg, (70%).

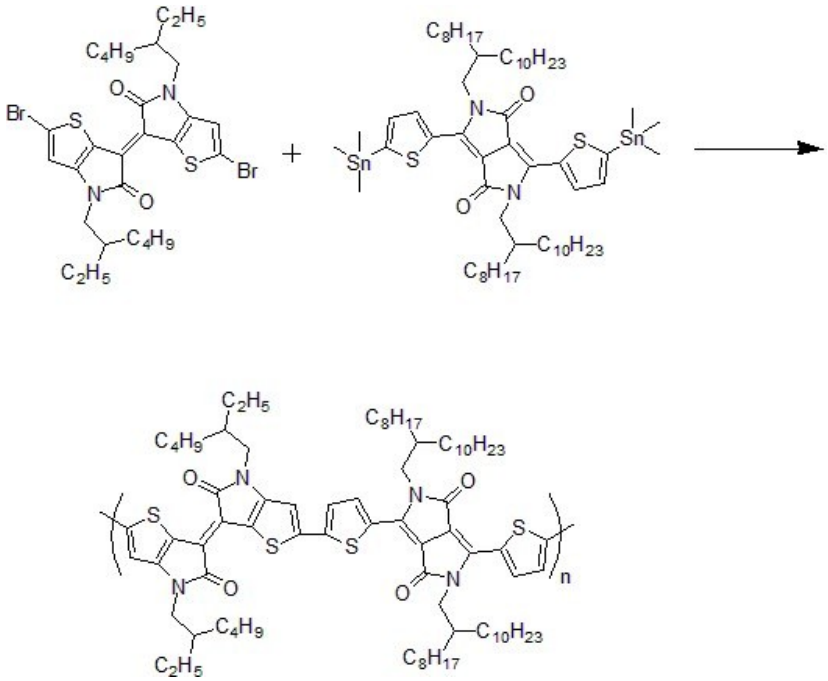

Scheme S2 The synthetic route of SP2.

Synthesis of Conjugated Copolymer SP3

As synthesis of SP1, same methods were used to prefabricate SP3. Now, monomer 3 (0.1 mmol, 35.2 mg) and monomer 4 (0.1 mmol, 118.7 mg) were used as monomers. The resulting polymer SP3 was dark solid, yield: 78 mg, (72%)

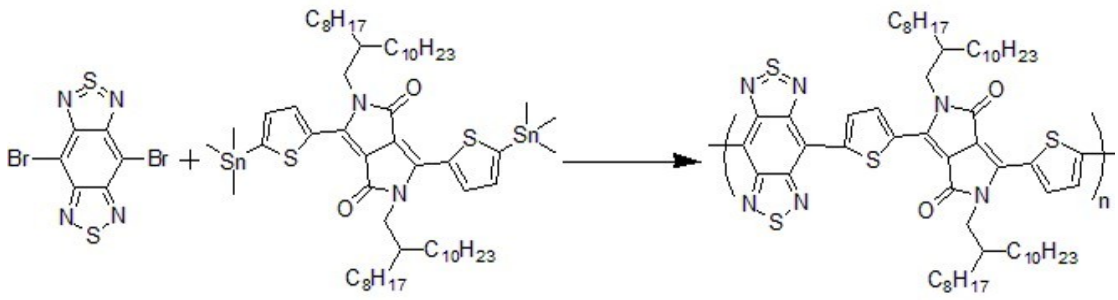

Scheme S3 The synthetic route of SP3.

Preparation of SPNs

All PEG-Encapsulated semiconducting polymers NPs (SPNs) were prepared with nanoprecipitation methods. Firstly, the semiconducting polymers (0.5 mg) and amphiphilic polymer (Pluronic F-127, 15 mg) were dissolved in THF (2 ml) and deionized water (10 ml), respectively. Then the solution dissolved semiconducting polymers was rapidly injected into deionized water with ultrasonication. After nanoprecipitation, THF was fully evaporated under vacuum at 45 ℃. Next, in order to purity and modulate the size of particles, aqueous solutions were filtered through a polyethersulfone (PES) syringe driven filter (0.45 μm) (Millipore). Then monodisperse solution was centrifuged and washed with deionized water for three times using a 100 K centrifugal filter units (Millipore) under centrifugation at 2,800 rpm for 10 min. The final SPNs solutions were collected and stored in 4 ℃ environment.

Characterizations

Nuclear magnetic resonance (NMR) spectra of the three semiconducting polymers was recorded on Bruker Ultra Shield Plus 400 MHz spectrometer, which used tetramethylsilane (TMS) and $CDCl_3$ as the internal reference and the deuterated solvent, respectively. Gel permeation chromatography (GPC) were carried out on Shim-pack GPC-80 X columns with THF as the eluent. The UV-VIS-NIR absorption spectra were recorded on a Shimadzu UV-3600 Plus UV-VIS-NIR spectrophotometer at room Temperature. Dynamic light scattering (DLS), a commercial laser light scattering spectrometers (ALV/CGS-3; ALV, Langen, Germany) at a scattering angle of 90° equipped with a multi-τ digital time correlator and a He–Ne laser (at λ = 632.8 nm), was used to characterize the average size and size distribution of SPNs. A CONTIN analysis was used to extract the $\langle R_h \rangle$ data (from the scattering intensity). When preparing the samples, the 0.45 μm Millipore filters were used to ensure the samples pure. All experiments were operating at room temperature and repeated for three times. Transmission electron microscopy (TEM) images were obtained from transmission electron microscope (HT7700) with an operational voltage of 100 kV. The 3-(4,5-dimethylthiazol-2-yl)-2,5-diphenyltetrazolium bromide (MTT) assay was carried out by a Power Wave XS/XS2 microplate spectrophotometer (BioTek, Winooski, VT). The

Olympus Fluoview FV1000 laser scanning confocal (Tokyo, Japan) was used to acquire confocal laser scanning microscopy (CLSM) cells images. Flow cytometry experiments were performed by Flow Sight Imaging Flow Cytometer (Merck Millipore, Darmstadt, Germany). The photothermal performance of the conjugated polymers and all photothermal tests were studied by Fotric 225 (Infrared thermoviewer) diwas, purchased from Fotric. (Shanghai, China). The photoacoustic experiments were carried out using the Vevo LAZR-X imaging instrument.

Cell Lines and Cell Culture

Key-gen Biotech Co. Ltd (Shanghai, China) sold us the Murine breast adenocar-cinoma cell line 4T1. 4T1 cells were incubated in complete Dulbecco's Modified Eagle Medium (DMEM) cell culture medium containing 10% fetal bovine serum (FBS) under the conventional environment (37 °C, 5% CO_2).

Animal Model

All animal experiments were in accordance with the NIH guidelines for the care and use of laboratory animals(NIH Publication no. 85-23 Rev. 1985) and approved by the Animal Ethics Committee of Simcere Bio Tech Corp., Ltd. Female BALB/c mice (5-6 weeks old) were purchased from Shanghai Laboratory Animal Center, Chinese Academy of Science (SLACCAS).To establish a tumor model, 4T1 cells suspended in 50 μL PBS (4×10^6) were subcutaneous injected into the left armpit of each mice. Tumor volume was about 120 ~ 200 mm^3 before being used for PA imaging and photothermal treatment.

***In Vitro* Photothermal Performance of SPNs**

SPNs2 and SPNs3 in aqueous solution with 25 μg mL^{-1} were irradiated by a 1064 nm laser for 8 min at 0.5 and 1.0 W cm^{-2} and SPNs1 with the same concentration was irradiated with a 915 nm laser for the same time at 0.5 W cm^{-2}. The thermal images and temperature changes were recorded every 30 s by an infrared camera (Fotric 225, Shanghai, China) until reaching room temperature. Photothermal conversion effiency (η) was calculated in accordance with the previous study under 915 nm laser at 0.5 W cm^{-2} or 1064 nm laser at 1 W cm^{-2}.

The photostability of SPNs was studied by monitoring photothermal performance

after five cycles of on/off 1064 nm or 915 nm laser irradiation, which were all at the MPE power density (1.0 W cm^{-2} or 0.5 W cm^{-2}), respectively. Briefly, the SPNs solutions were irradiated by laser for 5 min, followed cooling to room temperature for 3 min, which were repeated for 5 times.

***In Vitro* Deep-tissue Photothermal Effect in NIR-I and NIR-II Windows**

The photon in NIR-II windows can achieve larger tissue penetration depth compared to NIR-I window, as the result of lower scattering of tissue in this spectrum range. We choose chicken breast muscles as the model biological tissue and prepared different thickness (0, 5, 10, 15, 20 mm). The 100 L solution of SPNs (50 μg mL^{-1}), added in a 200 μL tube, were covered with tissues of different depths and then were subjected to 915 nm (SPNs1) and 1064 nm (SPNs2 and SPNs3) laser irradiation at 0.5 W/cm^2 and 1.0 W cm^{-2}, respectively. We studied the deep-tissue photothermal effect by recording temperature changes of SPNs3 solution captured using the thermal imaging camera.

***In Vitro* Cytotoxicity Assay**

The *in vitro* cytotoxicity of SPNs was studied by MTT assay in 4T1 cells. The cells were seeded in 96-well plates (Costar, IL, USA) at a density of 2×10^4 cells/well and incubated for 24 h under standard conditions (37 ℃, 5% CO_2). Different concentrations of SPNs3 (100 μL) were diluted in DMEM and added to wells. The cells were incubated containing SPNs solutions for 24 h without light. After that, the culture medium was replaced by fresh DMEM containing MTT (5 mg mL^{-1}). After another 4 h incubation, the culture medium was removed and replaced by 150 μL DMSO. The plates were gently shaken for 10 min to mix all of the precipitates formed. Finally, a PowerWave XS/XS2 microplate spectrophotometer was carried out to determine the absorption of 490 nm to evaluate relative cell viability.

***In Vitro* Photothermal Ablation of Cells**

4T1 cells were seeded in 96-wells plates at a concentration of 2×10^4 cells mL^{-1}. After 24 h incubation at 37 ℃, the DMEM containing different concentration of SPNs3 were added to wells and the cells were incubated for another 4 h. Then, the suspensions

were replaced by fresh DMEM and exposed to 1064 nm laser light for 5 min with a MPE power density (1 W cm^{-2}). After the cells were cultured for an additional 24 h, the MTT assay was used to evaluate the viability of cells

Cell Apoptosis Assay by Flow Cytometry

4T1 cells were seeded in 6-well plates (2 × 10^5 cells $well^{-1}$) and incubated with DMEM (containing 10% FBS) for 24 h. Then the culture medium was replaced by fresh DMEM containing of SPNs3 (25 μg mL^{-1}) and continuously cultured under standard condition. After 4 h incubated, the suspensions were removed and fresh medium were added to wells. Then the treating cells were irradiated with 1064 nm laser light at 1 W cm^{-2} for 5 min. After cultured for an additional 12 h, the culture medium was removed. The cells were washed softly with PBS and then harvested by trypsin treatment. Next, the cells were washed by PBS three times gently followed by staining with Annexin V-FITC/ propidium iodide (PI). Flow cytometry assay was performed via BD FACSCSanto flow cytometry.

Photothermal Effect *In Vitro* by Confocal Imaging

4T1 cells were seeded in single-well confocal dishes at a concentration of 1 × 10^5 cells mL^{-1}. After a 24 h incubation under 37 ℃ in a humidified atmosphere of 5% CO_2, the cells were cultured with medium containing SPNs3 (25 μg mL^{-1}) for 4 h without light. Then the suspensions were replaced by fresh medium and selected dishes were exposed to 1064 nm laser light (1 W cm^{-2}) for 5 min. The cells were cultured for another 12 h and then stained with Calcein-AM/propidium iodide (PI) solution for 10 min. Finally, the cells were imaged by CLSM (Olympus Fluoview FV1000).

Blood Hematology and Biochemistry Analysis

Blood samples were collected from the fundus artery after injection of 150 μL of PBS and SPNs3 (1 mg mL^{-1}) solutions at 0, 7 and 14 days. The collected blood samples were centrifuged at 1200 rpm for 10 min and washed several times with PBS. Then, hepatic function markers (ALT and AST) and renal function markers (CRE and BUN) were measured and routine blood tests were performed to measure (WBC), red blood cell (RBC), hematocrit (HCT), hemoglobin (HGB), PLT (platelet), MCHC (mean hemoglobin concentration), mean corpuscular volume (MCV), and MCH (mean

corpuscular hemoglobin). The standard blood biochemical indexes including aspartate aminotransferase (AST), urea, creatinine, and alanine ALT were also examined.

***In Vitro* and *In Vivo* PA Imaging**

For *in vitro* PA imaging, a point-to-point method was used to collect the PA spectra of conjugated polymer in NIR-II windows. The PA signals of SPNs were excited by different wavelength (from 1200 nm to 1500 nm) of pulsed light and signals of SPNs were collected through the Vevo LAZR-X PA imaging instrument, which provided conditions for the following PA imaging tests. Then, the region of interest (ROI) analysis was used to measure PA signal intensities of SPNs and the recorded curve of PA signal intensity was considered as the PA spectrum. A similar method was utilized to obtain the concentration-dependent PA signals. In order to analyze the PA signal of deep tissue depths, the tube containing 1 mg mL^{-1} solution of SPNs were covered with different thickness of chicken tissue and then PA signals were measured.

For PA imaging in live body, 4T1-tumor-bearing mice were firstly injected intratumorally with SPNs (50 μL, 500 μg mL^{-1}), and the PA images of tumor were obtained under pulsed laser at different wavelength (1200 nm, 1300 nm and 1400 nm). To monitor the accumulation of SPNs in the tumor section, 4T1-tumor-bearing mice were injected with SPNs (100 μL, 1 mg mL^{-1}) through tail vein. After injection, the PA images of tumor section were acquired via PA instrument at different time points (0, 2, 5, 8, 10 and 12 h). At 24 h after injection of SPNs, the main organs (heart, liver, spleen, lung and kidney) were collected and imaged under 1280 nm pulsed laser.

***In Vivo* PTT in the NIR-I and NIR-II window**

To assess *in vivo* photothermal therapy effect in deep tissue, the BALB/c mice bearing 4T1 tumor on the left armpit were primarily intratumorally injected with 50 μL SPNs solutions (200 ug mL^{-1}). The top of the tumor was covered with a piece of chicken breast tissue (2 mm) to simulate the deep tissue condition. Then the tumors covered chicken breast tissue were exposed to 915 nm laser (0.5 W cm^{-2}) or 1064 nm laser (1 W cm^{-2}), respectively. An infrared camera (Fotric 225, Shanghai, China) was used to monitor the temperature variation of the tumor region. Afterword, the 4T1 tumor-bearing mice were used and were administered with SPNs solution (10 mg kg^{-1}) via tail

vein. At 10 h postinjection, tumor regions were exposed to 915 nm laser (0.5 W cm^{-2}) or 1064 nm laser (1 W cm^{-2}), respectively. Then the tissue of tumors at different depth (0, 2, 4, 6 and 8 mm from the top sections which were irradiated by lasers) were resected and staining with hematoxylin and eosin (H&E).

For *in vivo* PTT in NIR-II biowindows, the 4T1 tumor-bearing mice were intravenously injected with PBS or SPNs3 (10 mg kg^{-1}). After 10 h injection, an infrared camera was utilized to monitor the temperature variation of the tumor region with different treatments (irradiation with or without 1064 nm laser at 1 W cm^{-2} for 5 min). After the corresponding treatments, the volume of the tumors were conducted by a vernier caliper every 2 days during 15 days and calculated by the equation: tumor volume = (tumor length) × $(\text{tumor width})^2/2$. Simultaneously, the body weight of the mice with different treatments were measured to evaluate the health of every mouse. After 15 days, tumor tissues and other major organs (heart, liver, spleen, lung and kidney) were dissected and (H&E) staining analysis of them was conducted. The intact tumors in all groups were weighed and photographed.

Reference

1. B. Guo, Z. Sheng, D. Hu, A. Li, S. Xu, P. N. Manghnani, C. Liu, L. Guo, H. Zheng and B. Liu, *ACS Nano*, 2017, **11**, 10124-10134.
2. K. Pu, J. Mei, J. V. Jokerst, G. Hong, A. L. Antaris, N. Chattopadhyay, A. J. Shuhendler, T. Kurosawa, Y. Zhou, S. S. Gambhir, Z. Bao and J. Rao, *Adv. Mater.*, 2015, **27**, 5184-5190.
3. Y. Jiang, J. Li, X. Zhen, C. Xie and K. Pu, *Adv. Mater.*, 2018, **30**, e1705980.